The Nova Rate in the Large and Small Magellanic Clouds

James D. Neill

Department of Physics and Astronomy, University of Victoria, Elliott Building, 3800 Finnerty Road, Victoria, BC, V8P 5C2, Canada

neill@uvic.ca

Michael M. Shara

American Museum of Natural History, 79th and Central Park West New York, NY, 10024

mshara@amnh.org

and

Michael C. B. Ashley

School of Physics, Department of Astrophysics and Optics, University of New South Wales, Sydney, NSW 2052, Australia

m.ashley@unsw.edu.au

Received _____; accepted _____

Submitted to PASP

ABSTRACT

We report the preliminary results of an ongoing nova survey of the Large Magellanic Cloud (LMC). Using the 0.5 m Automated Patrol Telescope and the 0.45 m Robotic Optical Transient Search Experiment Telescope located at Siding Spring Observatory in Australia, we observed the LMC and the SMC in continuum light over a span of 2 years on 102 separate nights. Our frame limits typically reached 16.0 V magnitudes, over two magnitudes fainter than the apparent magnitude the faintest observed nova would obtain at maximum light if placed in the LMC (13.5 Vmag). We detected no novae in our survey. Monte Carlo simulations of erupting novae in the LMC, using real nova light curves, place an upper limit on the bulk nova rate in the LMC of < 2.3 novae yr^{-1}. An analysis of the nova citings in the literature places a lower limit on the bulk nova rate of > 0.5 novae yr^{-1}. Using these limits and the integrated B magnitude for the LMC and $B-K$ colors and extinctions, gives K-band luminosity specific nova rate limits for the LMC of > 1.2 and < 5.5 yr$^{-1}[10^{10}L_{\odot,K}]^{-1}$.

Subject headings: novae, cataclysmic variables — galaxies: individual (LMC, SMC)

1. Introduction

The nova rates in low-mass galaxies are highly uncertain, yet offer the key to understanding an emerging mystery in nova populations. Evidence is mounting that the nova rate per unit K-band light may be a universal quantity, independant of host galaxy properties such as total mass, metallicity, or star formation history (Shafter et al. 2000; Ferrarese et al. 2003). However, analyses of the spatial distributions of novae in disk galaxies containing both old and young populations indicate that only 10 to 30% of the novae in these galaxies can be associated with younger, recently star-forming populations in their disks (Ciardullo et al. 1987; Shafter & Irby 2001; Neill & Shara 2004) and therefore, the nova rate per unit light should be higher in galaxies dominated by older populations.

If the nova rate per unit light is a universal quantity, this would imply that novae can be used to accurately measure stellar light in diverse environments, e.g., between the galaxies of a cluster (Neill et al. 2005). It would also imply that the time required to begin producing novae in a given population is close to the star-formation timescale and that once novae are being produced they continue to be produced at the same rate even after star formation has stopped. Given that the Type Ia supernova rate is higher for late-type systems than early-type (Oemler & Tinsley 1979; van den Bergh & Tammann 1991; Mannucci et al. 2005) a universal nova rate per unit light would rule out classical novae as a progenitor population for Type Ia SNe (though recurrent novae may still play a role). If the nova rate per unit light is not universal, the trend must be measured in order to understand the factors influencing nova production.

The error bars on the nova rate per unit light are still large for most galaxies (Shafter et al. 2000). We claim that systematic errors due to incomplete spatial and sparse time sampling overwhelm the random errors in nova rates, and we have endeavored to improve this situation by using a comprehensive, densely time-sampled survey technique (Neill &

Shara 2004). Our study of M81, a large nearby spiral galaxy, produced a larger bulk rate than previously reported and revealed evidence for obscuration of novae in the inner bulge due to dust in the disk that extends into the nuclear region (Neill & Shara 2004), implying that even our higher rate is a lower limit.

One way forward is to determine accurate nova rates for simpler, lower-extinction systems, dominated by either old or young populations. We are fortunate that the local group offers nearby dwarf ellipticals (dEs) for sampling intermediate to older populations and nearby dwarf irregulars (dIs) with active star formation for sampling a younger population. The low mass of these systems provides a challenge for determining an accurate nova rate because they produce few novae per year and so a long term survey is required to achieve good statistics. Being nearby, these systems can be quite large on the sky and so require large field-of-view cameras to survey the systems comprehensively. In order to obtain accurate nova rates for these low-mass systems, a densely time-sampled survey must be conducted to minimize the uncertainties associated with correcting for the sparse time sampling afforded by most typical observing programs.

We have begun a program undertaking this challenge by focusing on four nearby systems; the dEs M32 and NGC 205 (Neill & Shara 2005), the Large Magellanic Cloud (LMC), and the Small Magellanic Cloud (SMC). The LMC is a very nearby ($(m - M)_0 = 18.50 \pm 0.02$, Alves 2004) satellite dI of the Milky Way with active star formation and relatively low internal extinction ($A(B)_i = 0.07$, de Vaucouleurs et al. 1991, herinafter RC3). Our program will span several years and will montitor each of these galaxies comprehensively each clear night over significant fractions of a year to determine the most accurate nova rates to date for these systems. The preliminary results from the first observing season for M32 and NGC 205 are reported in Neill & Shara (2005). Here we report the preliminary results from our first season observing the LMC.

2. Observations

All images for this survey were taken with the Automated Patrol Telescope (APT), a robotically controlled telescope located at Siding Spring Observatory in New South Wales, Australia (Carter et al. 1992). The APT is a modified Baker-Nunn camera with a 0.5 m clear aperture. The imager uses an EEV CCD chip with 1152 × 770 pixels, each 22.5μ across, which gives a scale on the sky of 9.″4 per pixel. The resulting field of view is 2.°9 × 1.°9 and required modifying the optics of the camera to produce a flat field over this area (Carter et al. 1992). The filters for the APT are mounted between the CCD and the primary mirror, making filter changes difficult. The V-band filter was chosen because it was compatible with other programs being carried out on the APT during our survey. The V-band filter facilitates a comparison with the extensive database of continuum nova light curves available in the literature (Arp 1956; Rosino 1973) and is also compatible with our nova survey of local group dEs (Neill & Shara 2005).

Figure 1 illustrates the coverage of the LMC by the APT. Six fields covering roughly 30 square degrees were required and are labeled on the figure. Each individual exposure was 60 seconds and from two to six exposures were taken on each epoch. The effect of seeing variations were minimized by the large pixel scale of the APT and camera. Cosmic rays were rare because of the short exposure time employed.

The observations spanned the range from 2004 January 17 to 2004 April 23 (MJD 53021.93 to 53118.87), a total of 96.94 days. During this span we were able to acquire epochs of each of the six fields on 46 nights. The remaining 51 nights were lost due to bad weather, full moon, or minor equipment problems. Table 1 summarizes the observations.

3. Reductions

The bias for each APT image was calculated from the 50 pixel wide overscan region and subtracted. Twilight flats were used to remove the overall instrumental response and pixel-to-pixel sensitivity variations.

The individual frames for each epoch were then measured with DAOPHOT II, registered to a standard epoch with **daomatch** and **daomaster**, and combined using **montage2** (Stetson 1987) using a median stack. This removed the few cosmic rays from the final epoch image and improved the signal-to-noise ratio. The standard epoch used for the positional registration was taken at the start of the run on MJD 53021.93. This epoch had at least four exposures per field and had excellent image quality.

4. Photometry

We used the DAOPHOT II aperture photometry routine (Stetson 1987) to detect and measure point sources in our combined epoch images. The measurement aperture for each image was 1.3 pixels in radius, corresponding to 12.2 arcseconds on the sky. The background was measured using a sky annulus with radii of 5 to 15 pixels around each object.

To calibrate our photometry we compared our instrumental magnitudes with the V-band photometry of the LMC by Zaritsky et al. (2004). We used from 1700 to 2400 objects per field to determine a photometric offset to apply to our instrumental magnitudes to bring them onto the standard V-band system. The uncertainty in this offset ranged from 0.002 to 0.003 magnitudes after a 2σ cut was applied to trim outliers.

Figure 2 shows the offset between our instrumental magnitudes and the calibrated magnitudes of Zaritsky et al. (2004) for one of our LMC fields. Even though the uncertainty in the mean is small, by virtue of the large numbers of reference stars, the RMS of the

scatter about the mean is a much larger 0.1 magnitudes. This is due to the undersampling of the stellar point-spread-function (PSF) by the large pixels. The brightness of the star varies depending where on the pixel it falls.

We used DAOPHOT II to derive a point-spread-function (PSF) for each image and then add artificial stars to determine the frame limit for each epoch. The frame limit was defined as the point at which fewer than 50% of the artificial stars were recovered in our blinking process. We present histograms of the frame limits for each field in Figure 3 from which it can be seen that the frame limits range from 15.4 to 16.6 V magnitudes. This range is primarily due to variations in transparency, exposure time, and crowding for each field.

5. Nova Detection

With a distance modulus to the LMC of 18.50 (Alves 2004), the faintest novae, at $M_V = -5.1$ (Neill & Shara 2005), would reach an apparent V magnitude of 13.4. The brightest novae ($M_V = -10.0$) would reach 8.5 V magnitudes. This range is 2.0 magnitudes brighter than the shallowest epoch frame limit for this survey (see above). Our nova candidate criteria require that the candidate be transient and that it be visible on more than one epoch (to avoid spurious detections caused by imperfectly removed cosmic rays). To further discriminate against cosmic rays, we require that a candidate be visible on each of the individual frames for the given epoch as well as the combined epoch image.

We blinked each image against the standard epoch to look for changing point sources and found no nova candidates. In addition to this blinking process, we also analyzed the light curves of each point source down to V of 16.5 to find possible slow nova candidates. We analyzed roughly 90,000 point sources and found numerous variable stars, but no object

with a monotonically decreasing light curve like a slow classical nova on the decline.

6. The Nova Rate: an Upper Limit

Having detected no novae, we can only place an upper limit on the nova rate in the LMC. A raw limit can be derived by taking the inverse of the survey time in years which yields $R \leq 1/0.26 = 3.8$ novae yr^{-1}.

6.1. The Monte Carlo Approach

To improve on this estimate of the nova rate in the LMC, we can use a sample of continuum nova light curves from Arp (1956) and Rosino (1973), combined with our individual epoch frame limits, to perform a Monte Carlo simulation of erupting novae in the LMC. This technique was first described in Shafter & Irby (2001) and our modifications to this method, which include using the individual epoch frame limits, are described in Neill & Shara (2004, 2005).

This technique makes many independent estimates of the observed nova rate in the given galaxy as a function of the true nova rate [$R_{obs}(R_t)$]. For a given trial estimate of R_t, the true rate, we choose a random set of novae (which specify the maximum magnitudes and decline rates of real novae) and a random set of outburst times. We then pick a random field for each nova which determines which frame limits are used to calculate the number of observed novae using the candidate criteria described above. We repeat this 10^5 times and record how many times our simulation matches the number of nova candidates actually observed in the survey (0). The estimate of the true nova rate R_t is then incremented and the process is repeated until the number of matches goes to zero. This produces a probability distribution for R_t (see Figure 4). The best estimate for R_t is that which

corresponds to the peak of this distribution.

Figure 4 shows the probability distribution for our survey of the LMC. The range encompassing half of the probability distribution near the peak is indicated by the solid horizontal line and defines the upper limit for the bulk nova rate for the LMC of 2.3 novae yr^{-1}.

7. The Nova Rate: a Lower Limit from the Literature

We can place a lower limit on the nova rate in the LMC by examining the historical record of nova detections in the literature. We used the list of LMC novae reported in Subramaniam & Anupama (2002) along with recent reports of novae in the LMC from the International Astronomical Union Circulars (IAUC). We removed the recurrent nova reported in 1968 and 1990, and the recurrent nova reported in 1937, and 2004. Figure 5 shows a histogram of the classical novae reported in the LMC as a function of time. We also plot a running average nova rate using a window that includes the previous 20 years from the date plotted as a dashed line.

Without making any corrections for completeness, we can see that since 1980, the 20 year average nova rate has been close to 0.5 yr^{-1}. In an attempt to account for incompleteness, since most of these novae were discovered serendipitously, we could claim that the peak in 1989 of 0.7 yr^{-1} represents the best lower limit on the nova rate in the LMC. We will instead be conservative and use the average value since 1980 of 0.5 yr^{-1} as our lower limit on the bulk nova rate in the LMC.

Both these limits are consistent with the rate previously reported by Capaccioli et al. (1990) of $\sim 2 \pm 1$ yr^{-1}, determined purely from the LMC novae reported in the literature up to 1990 and making statistical corrections for completeness. It is also consistent with the

rate reported by Graham (1979) of 2.5 ± 0.5 yr^{-1}, determined from a sparsely time-sampled photographic survey spanning the 1970s.

7.1. The Luminosity Specific Nova Rate

It is standard practice to normalize a nova rate using an infrared luminosity to allow the inter-comparison of rates from a wide range of galaxy types. Optical or blue luminosity normalizations are subject to large variations due to a few young stars, while the IR is not subject to these variations and is, therefore, a more stable indicator of a galaxy's total mass (see, e.g., Neill & Shara 2005).

We start with the integrated B magnitude, $B-V$ color, and extinction estimates for the LMC from the RC3 and Schlegel et al. (1998). To derive a K-band integrated magnitude, we must also use the $V-K$ color from Aaronson (1978). We apply these numbers using the following formula:

$$K_{int} = B_{int} - [A(B)_i + A(B)_g] - [(B-V)_0 + (V-K)_0], \quad (1)$$

where $A(B)_i$ is the extinction internal to the LMC, $A(B)_g$ is the Galactic extinction toward the LMC, and all units are magnitudes. Using, $B_{int} = 0.91 \pm 0.05$, $B-V = 0.44 \pm 0.03$, $A(B)_i = 0.07$ from the RC3, $A(B)_g = 0.32$ from Schlegel et al. (1998), and $V-K = 2.30 \pm 0.10$ from Aaronson (1978), we get an integrated K-band magnitude for the LMC of $K_{LMC,int} = -2.22 \pm 0.12$. We use a distance modulus to the LMC of 18.50 ± 0.02 (Alves 2004) to convert this to an integrated absolute K-band magnitude, which gives $M_K = -20.72 \pm 0.18$. We compare this with the solar absolute K-band magnitude, $M_{\odot,K} = 3.33$ (Cox 2000), to derive the K-band luminosity of the LMC in units of $10^{10} L_{\odot,K}$: $L_{LMC,K} = 0.42 \pm 0.07 [10^{10} L_{\odot,K}]$. We then divide our upper limit by

this luminosity to get an upper limit on the luminosity specific nova rate (LSNR) in the LMC: $LSNR_K < 2.3\ \mathrm{yr}^{-1}/0.42 \pm 0.07[10^{10}L_{\odot,K}] = 5.5\ \mathrm{yr}^{-1}[10^{10}L_{\odot,K}]^{-1}$. Our lower limit becomes: $LSNR_K > 0.5\ \mathrm{yr}^{-1}/0.42 \pm 0.07[10^{10}L_{\odot,K}] = 1.2\ \mathrm{yr}^{-1}[10^{10}L_{\odot,K}]^{-1}$.

8. Discussion

This range for the LSNR of the LMC overlaps the universal value derived from higher-mass galaxies of $1.71 \pm 0.61\ \mathrm{yr}^{-1}[10^{10}L_{\odot,K}]^{-1}$ reported in Ferrarese et al. (2003). Comparing the LMC LSNR range with the LSNR derived for the local dEs of $14.1^{+14.8}_{-4.9}$ $\mathrm{yr}^{-1}[10^{10}L_{\odot,K}]^{-1}$ (Neill & Shara 2005), we see an offset of 1.8σ between the two rates. Even though this difference is small, it is tantalizing. One more season will improve the statistics enough to determine if this offset is real.

9. Conclusions

We observed over 30 square degrees centered on the LMC in the V-band for 46 nights over a span of 97 nights and discovered no nova candidates.

1. Using Monte Carlo simulations, we derive an upper limit on the bulk nova rate in the LMC of 2.3 yr^{-1}.

2. Using novae reported in the literature, we derive a lower limit on the bulk nova rate in the LMC of 0.5 yr^{-1}.

2. Using B integrated magnitudes and $B-K$ colors and extinctions, we constrain the K-band LSNR for the LMC to be between 1.2 and 5.5 $\mathrm{yr}^{-1}[10^{10}L_{\odot,K}]^{-1}$.

We would like to acknowledge the invaluable efforts of Marton Hidas, Jessie

Christiansen, Stephen Crothers, Andre Phillips, and John Webb, who assisted us with the APT observations.

REFERENCES

Aaronson, M. 1978, ApJ, 221, L103

Alves, D. R. 2004, New Astronomy Review, 48, 659

Arp, H. C. 1956, AJ, 61, 15

Capaccioli, M., della Valle, M., D'Onofrio, M., & Rosino, L. 1990, ApJ, 360, 63

Carter, B. D., Ashley, M. C. B., Sun, Y.-S., & Storey, J. W. V. 1992, Proceedings of the Astronomical Society of Australia, 10, 74

Ciardullo, R., Ford, H. C., Neill, J. D., Jacoby, G. H., & Shafter, A. W. 1987, ApJ, 318, 520

Cox, A. N. 2000, Allen's astrophysical quantities (Allen's astrophysical quantities, 4th ed. Publisher: New York: AIP Press; Springer, 2000. Editedy by Arthur N. Cox. ISBN: 0387987460)

de Vaucouleurs, G., de Vaucouleurs, A., Corwin, H. G., Buta, R. J., Paturel, G., & Fouque, P. 1991, Third Reference Catalogue of Bright Galaxies (Volume 1-3, XII, 2069 pp. 7 figs.. Springer-Verlag Berlin Heidelberg New York)

Ferrarese, L., Côté, P., & Jordán, A. 2003, ApJ, 599, 1302

Graham, J. A. 1979, in IAU Colloq. 46: Changing Trends in Variable Star Research, 96–+

Mannucci, F., della Valle, M., Panagia, N., Cappellaro, E., Cresci, G., Maiolino, R., Petrosian, A., & Turatto, M. 2005, A&A, 433, 807

Neill, J. D. & Shara, M. M. 2004, AJ, 127, 816

—. 2005, AJ, 129, 1873

Neill, J. D., Shara, M. M., & Oegerle, W. R. 2005, ApJ, 618, 692

Oemler, A. & Tinsley, B. M. 1979, AJ, 84, 985

Rosino, L. 1973, A&AS, 9, 347

Schlegel, D. J., Finkbeiner, D. P., & Davis, M. 1998, ApJ, 500, 525

Shafter, A. W., Ciardullo, R., & Pritchet, C. J. 2000, ApJ, 530, 193

Shafter, A. W. & Irby, B. K. 2001, ApJ, 563, 749

Stetson, P. B. 1987, PASP, 99, 191

Subramaniam, A. & Anupama, G. C. 2002, A&A, 390, 449

van den Bergh, S. & Tammann, G. A. 1991, ARA&A, 29, 363

Zaritsky, D., Harris, J., Thompson, I. B., & Grebel, E. K. 2004, AJ, 128, 1606

This manuscript was prepared with the AAS LaTeX macros v5.2.

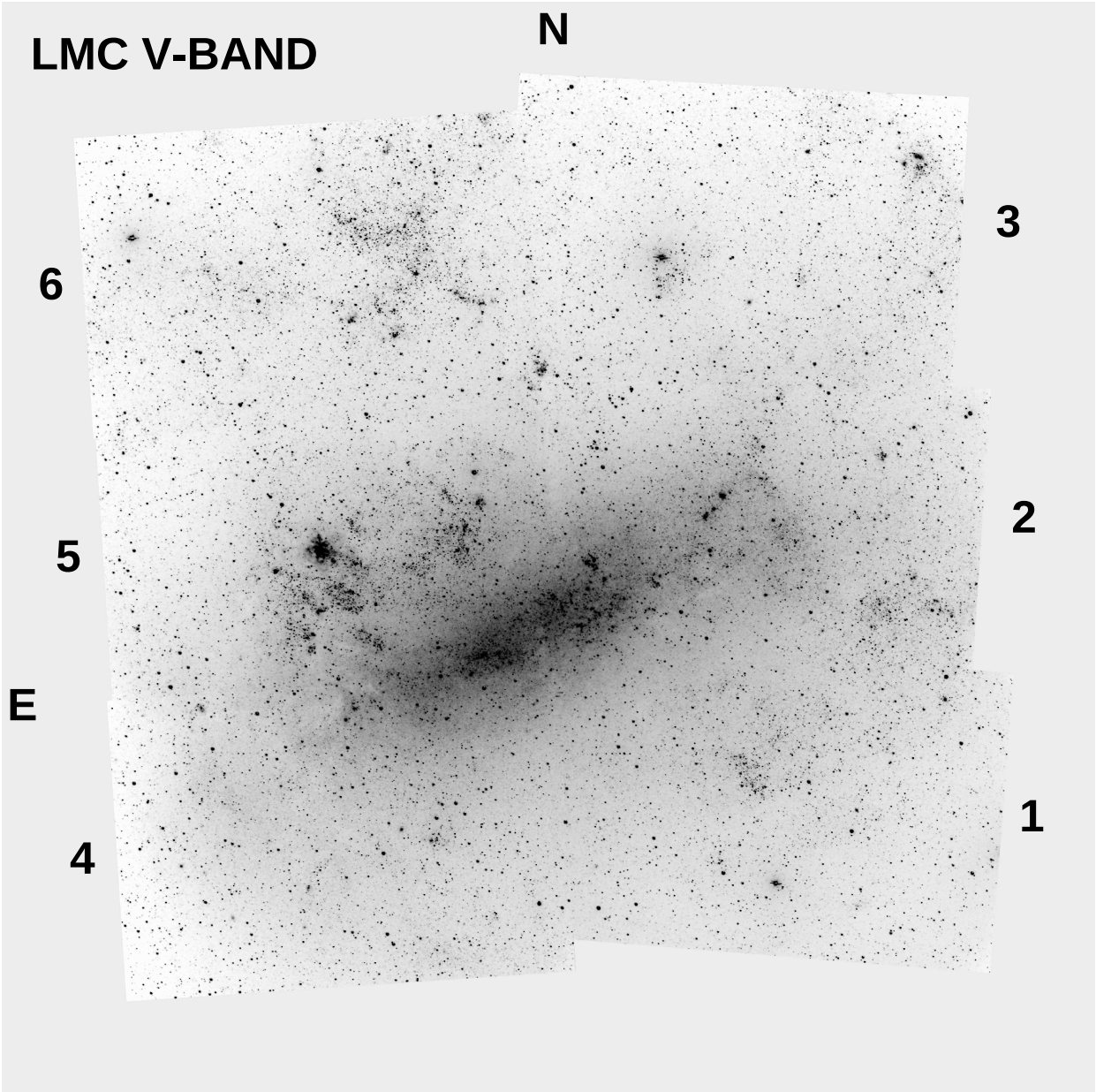

Fig. 1.— LMC survey area in the V-band. The field of view is approximately 5.5 degrees on a side covering more than 30 square degrees. This image was produced by coadding all but a few epochs of the entire survey. North is up and east left, as indicated. The field numbers are labeled on the outside edge of the six fields.

Fig. 2.— Instrumental V-band magnitudes minus calibrated V-band magnitudes from Zaritsky et al. (2004) versus calibrated magnitude. The full line shows the mean offset which is noted on the plot along with the uncertainty in the mean. The dashed lines show the sigma of the scatter about the mean, due to the severe PSF undersampling by the 9.4 arcsecond pixels.

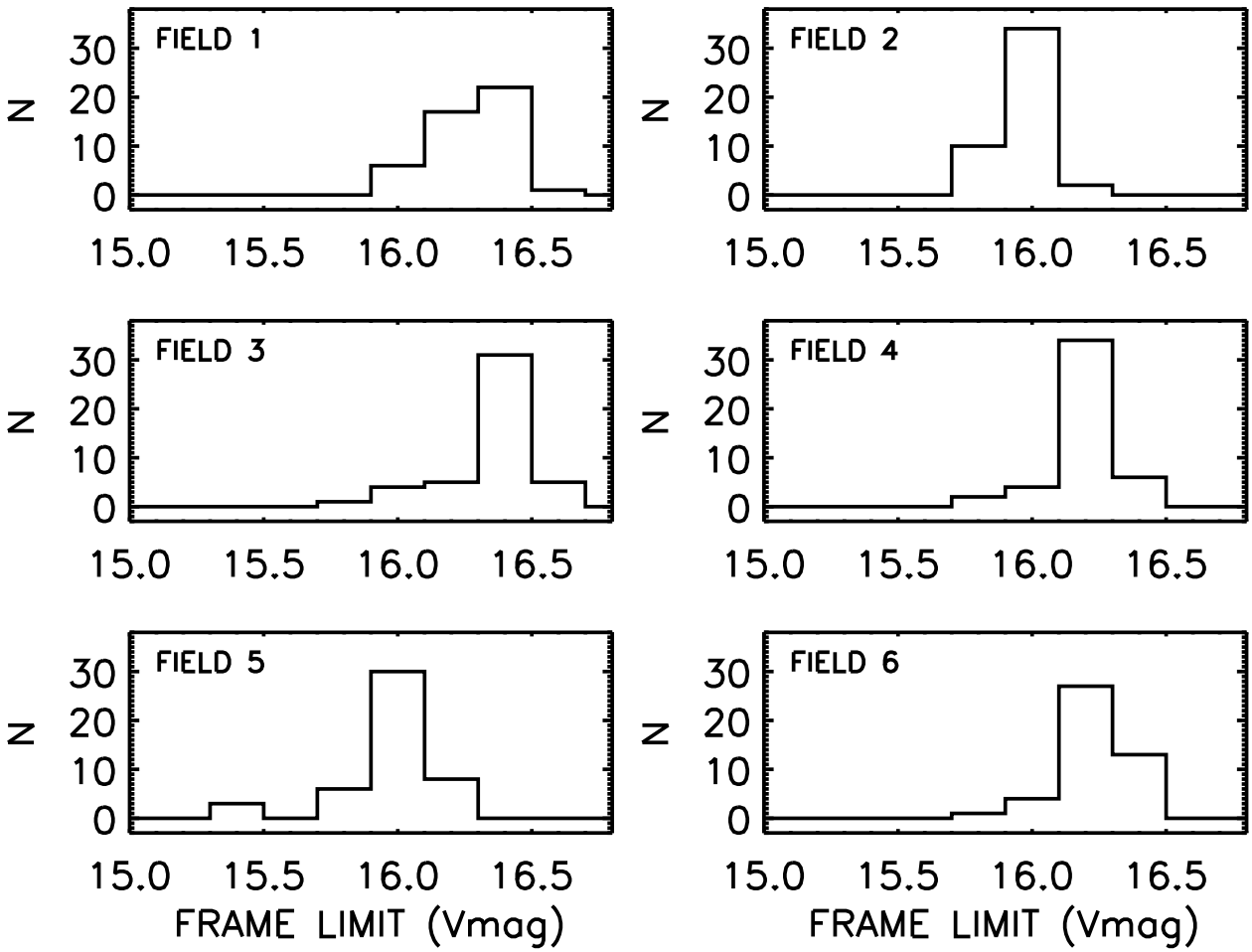

Fig. 3.— Histograms of the frame limits as determined by artificial star experiments for the six fields covering the LMC. The limits range from 15.4 to 16.6 V magnitudes, while the peaks of the distributions are all 16.0 V magnitudes or fainter.

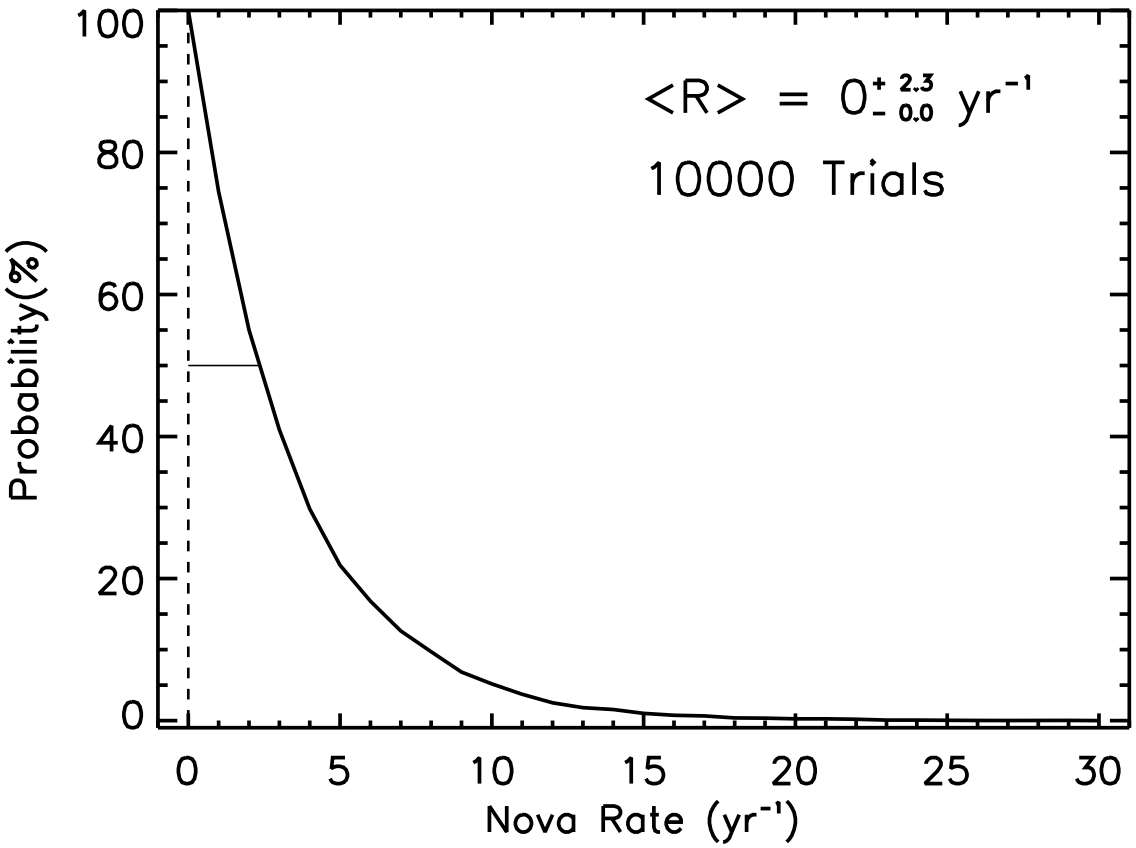

Fig. 4.— Probability distribution from Monte Carlo simulations of erupting novae in the LMC. The most probable value is 0 yr^{-1}, but 50% of the distribution is included up to a rate of 2.3 yr^{-1}, which defines the upper limit on the bulk nova rate in the LMC.

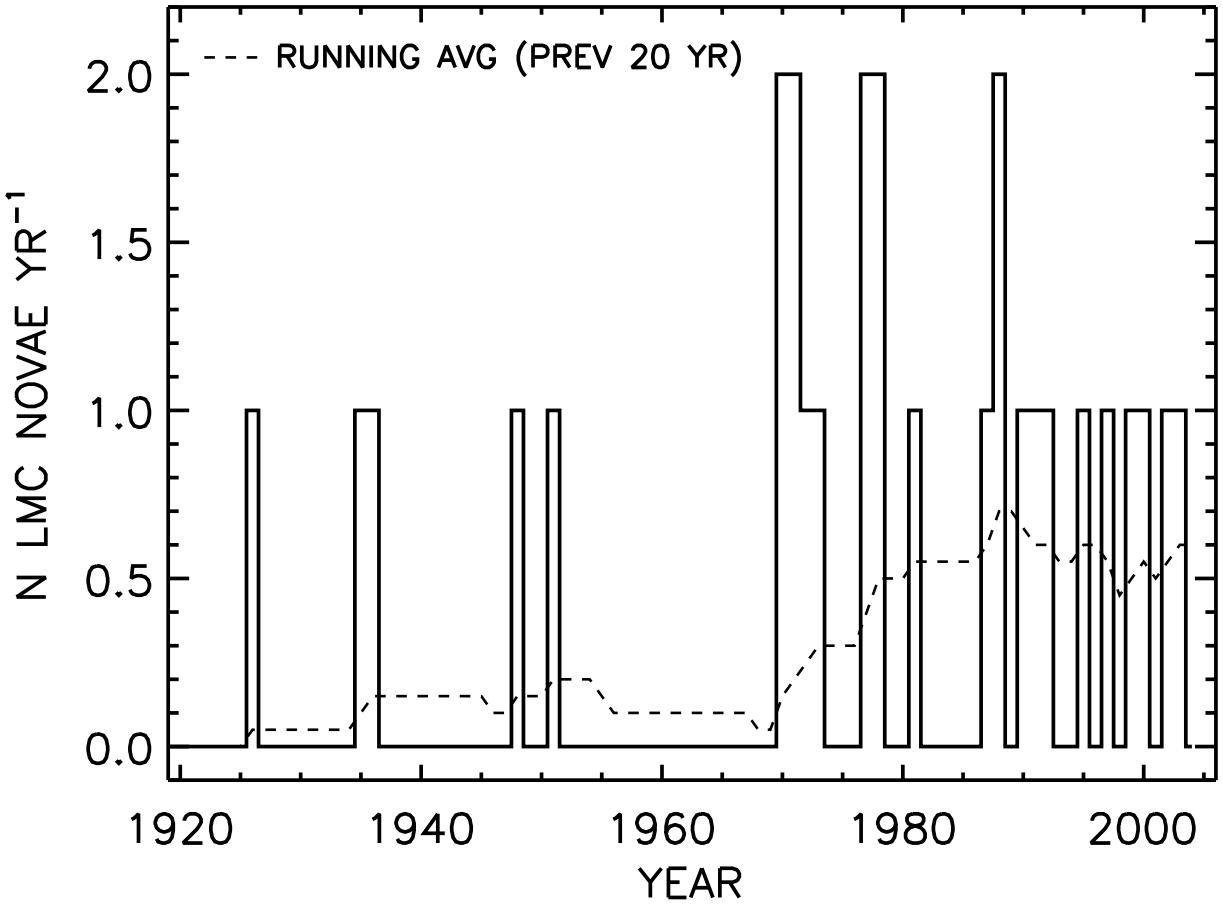

Fig. 5.— Histogram of LMC nova detections as a function of year plotted as a solid line. The running average nova rate for the 20 years previous to the point plotted is shown as a dashed line.

Table 1. APT V-band Observations

Epochs (N)	Exp. (s)	Start (MJD)	End (MJD)	Span (days)	Novae (N)
46	120-360	53021.93	53118.87	96.94	0